

MICROSTRUCTURAL EXAMINATION OF V-(4-5%)Cr-(4-5%)Ti Irradiated in X530 - D. S. Gelles (Pacific Northwest National Laboratory)^a and H. M. Chung (Argonne National Laboratory)

OBJECTIVE

The objective of this effort is to provide collaborative understanding of microstructural evolution in irradiated vanadium alloys for first wall applications in a fusion reactor.

SUMMARY

Microstructural examination results are reported for two heats of V-(4-5%)Cr-(4-5%)Ti irradiated in the X530 experiment to ~4 dpa at ~400°C to provide an understanding of the microstructural evolution that may be associated with degradation of mechanical properties. Fine precipitates were observed in high density intermixed with small defect clusters for all conditions examined following the irradiation. The irradiation-induced precipitation does not appear to be affected by preirradiation heat treatment at 950-1125°C. There was no evidence for a significant density of large (diameter >10 nm) dislocation loops or network dislocations.

PROGRESS AND STATUS

Introduction

Vanadium-based alloys are being developed for application as a first wall material for magnetic fusion power system. It has been shown that alloys of composition V-(4-5%)Cr-(4-5%)Ti have very promising physical and mechanical properties.¹ Recent attention in this alloy class has focused on several issues, such as the effect of low-temperature irradiation on fracture toughness, the effect of helium generation, the effect of minor impurities, and heat-to-heat variation in work-hardening behavior at low irradiation temperatures. While other classes of alloys are still considered, the V-(4-5%)Cr-(4-5%)Ti alloys are being optimized to suppress their susceptibility to loss of work-hardening capability following irradiation at low temperatures. Susceptibility of the alloy class to this process under fusion-relevant helium-generating conditions is considered to be a major factor in governing the minimum operating temperature of magnetic fusion devices.

Recent irradiation experiments at <430°C have shown that the loss of work-hardening capability and uniform elongation of V-4Cr-4Ti vary strongly from heat to heat and are influenced significantly by helium generated in the alloy.² The present effort was initiated to provide an understanding of the microstructural evolution in some heats of the V-(4-5%)Cr-(4-5%)Ti class that correspond to specimens with degradation of mechanical properties.² Specifically, two issues were addressed: the microstructural characteristics of a 500-kg heat of V-4Cr-4Ti (Heat #832665, referred to in reference 3 as BL-71) not previously examined following irradiation, and the cause of degraded properties in both an 80-kg heat of V-5Cr-5Ti (Heat BL-63) and the 500-kg heat following irradiation at ~385°C to ~4 dpa in the X530 experiment in EBR-II. In contrast to a 100-kg heat of V-4Cr-4Ti (Heat VX-8), the 500-kg heat did suffer from virtual loss of work-hardening capability during the irradiation.²

^aOperated for the U.S. Department of Energy by Battelle Memorial Institute under Contract DE-AC06-76RLO 1830.

Experimental Procedure

Specimens in the form of microscopy disks 3 mm in diameter were included in the X530 experiment. Five samples were selected for examination comprising two heats of material but each with a different preirradiation heat treatment condition. The compositions of the heats are given in Table 1^{3,4} and the specimen conditions are shown in Table 2. Specimens of BL-63 had been included in capsule S8 and specimens of BL-71 had been included in capsule S9 of the X530 experiment⁵ which achieved an exposure of 35 effective full power days yielding a peak fluence of 7.3×10^{21} n/cm² ($E > 0.1$ MeV) corresponding to damage of ~ 4 dpa.⁶ The capsules also contained matching miniature tensile specimens of the same conditions. The bottom of capsule S8 was 9.80 inches from the bottom of the core and the bottom of capsule S9 was 7.35 inches above the bottom of the core upon which actual irradiation temperatures and doses have been estimated and included in Table 2.^{7,8} One specimen of each of the BL-71 conditions was electrolytically thinned at ANL following irradiation, and one specimen of each of the BL-63 conditions was thinned at PNNL. Specimen BL-71-WR1050 was briefly repolished at PNNL. Examinations were performed on JEOL 1200EX and 2010F analytical transmission microscopes. Image processing from negatives was entirely by computer, with some minor loss in resolution and contrast range.

Table 1. Composition of Heats Examined

Heat #	Nominal Composition, wt%	Minor Impurities [appm]				
		O	N	C	Si	Other
BL-63	V-4.6Cr-5.1Ti	440	28	73	310	200 Al
832665, BL-71	V-3.8Cr-3.9Ti	310	85	80	783	220 Fe, 190 Al

Table 2. Specimen and Irradiation Conditions for the X530 Experiment.

Specimen Designation	Preirradiation heat treatment	Fluence (n/cm ²)	Dose (dpa)	Temperature (°C)
BL-63-CR950	cold rolled, annealed at 950°C/1h	6.7×10^{21}	4.3	400.5
BL-63-CR1050	cold rolled, annealed at 1050°C/1h	6.7×10^{21}	4.3	400.5
BL-71-WR950	warm rolled, annealed at 950°C/1h	7.3×10^{21}	4.7	399.1
BL-71-WR1050	warm rolled, annealed at 1050°C/1h	7.3×10^{21}	4.7	399.1
BL-71-WR1125	warm rolled, annealed at 1125°C/1h	7.3×10^{21}	4.7	399.1

Results

Despite the limited number of samples available for examination, it was possible to provide useful observations for all sample conditions. Preirradiation heat treatment was verified based on grain size comparison. BL-63-CR950 had a grain size on the order of 10 μm , BL-63-CR1050 much greater than 10 μm , BL-71-WR950 between 2 and 10 μm , BL-71-WR1050 much greater than 5 μm , and BL-71-WR1125 between 20 and 80 μm . The microstructures of all conditions were as expected, showing large and intermediate sized (Ti, V) oxy-carbo-nitride particles randomly distributed, and small particles

decorating grain boundaries in the BL-71-WR1050 and BL-71-WR1125.⁹ Evidence for effects of irradiation could only be identified on a fine scale. Examples of each of these microstructures at low magnification are given in Figure 1.

Careful examination of diffraction information indicated enhanced scattering in two regions of reciprocal space: a radial streak in the 200 direction at approximately $\frac{3}{4}\langle 200 \rangle$ and a similar tangential streak at approximately $\frac{2}{3}\langle 222 \rangle$. Dark field imaging with each of these features showed similar but not identical distributions of fine features, assumed to be precipitates. As streaking is in different directions for each of these diffraction features, different populations of precipitates would be expected to be in contrast. Similar attempts to image the dislocation structure using weak beam conditions on matrix reflections gave very complex images with features of similar size to the precipitate features. It is therefore likely that several matrix reflections superimpose on precipitate reflections. It was possible to obtain precipitate dark field images for each sample condition using $\frac{3}{4}\langle 200 \rangle$ contrast in stereo by tilting on (200). Stereo model observations demonstrated that the precipitate features tended to form in layers distributed through the foil thickness, verifying that they were not surface artifacts. All specimens gave similar diffraction behavior. Examples of one dark field image for each sample condition using $\vec{g} = \frac{3}{4}\langle 200 \rangle$, and the accompanying bright field image are provided in Figure 2, cropped to show behavior at a grain boundary. Figure 2 also includes an example of the diffraction information, inset.

From Figure 2, it can be demonstrated that precipitation is very fine. For example, particles in Figure 2g are 2 nm long by 1 nm wide, the narrow dimension corresponding to the streaking in $\langle 200 \rangle$. It is surprising that such small particles can be successfully imaged. The precipitate dark field images appear to differ between the two heats, but the size distribution is invariant with respect to the preirradiation heat treatment. The exact nature of the differences between the precipitate morphologies for the two heats is difficult to quantify. Although the images of precipitates in BL-63 appear to be larger, careful examination of the negatives suggests that the larger particles are a result of rafts of closely spaced smaller particles, of similar size to those in BL-71. However, it can be argued that the particles are larger in BL-63, and the fine structure appears for other reasons.

Precipitate measurements based on foil thicknesses, measured stereographically, gave particle densities as follows; BL-63-CR950: 6.3 nm mean diameter at $4 \times 10^{17} \text{ cm}^{-3}$ for a volume fraction of 3.5%, BL-63-CR1050: 4.9 nm mean diameter at $2 \times 10^{17} \text{ cm}^{-3}$ for a volume fraction of 0.8%, BL-71-WR950: 4.4 nm mean diameter at $1.1 \times 10^{17} \text{ cm}^{-3}$ for a volume fraction of 0.3%, BL-71-WR1050: 4.8 nm mean diameter at $4 \times 10^{17} \text{ cm}^{-3}$ for a volume fraction of 1.3%, and BL-71-WR1125: 3.7 nm mean diameter at $3 \times 10^{17} \text{ cm}^{-3}$ for a volume fraction of 0.4%. These measurements should be considered estimates given the difficulty of the analysis, but they provide further indication that the precipitation found could be responsible for the observed irradiation hardening in BL-71, but do not explain the difference in behavior between the two heats.

Figure 2 also provides insights regarding irradiation response at grain boundaries. The grain boundary images for BL-63-WR950, BL-71-WR950 and BL-71-WR1050 in Figures 2b, f and h appear to show a coating on the boundary. Also, Figure 2g for BL-71-WR1050 shows larger precipitate particles at the grain boundary showing brightly under the same conditions as the fine precipitate, and therefore the two features may be related. Similar larger features can be seen in Figure 2j for BL-71-WR1125, and are expected to be remnants of the preirradiation heat treatment.⁸

Several attempts were made to obtain compositional information from the fine precipitate features. Difficulties were encountered identifying the exact location of a precipitate so that a 1 nm focussed spot could be positioned to obtain characteristic precipitate composition information. Techniques based on $\frac{3}{4}\langle 200 \rangle$ dark field imaging and lattice imaging to identify precipitate locations failed to

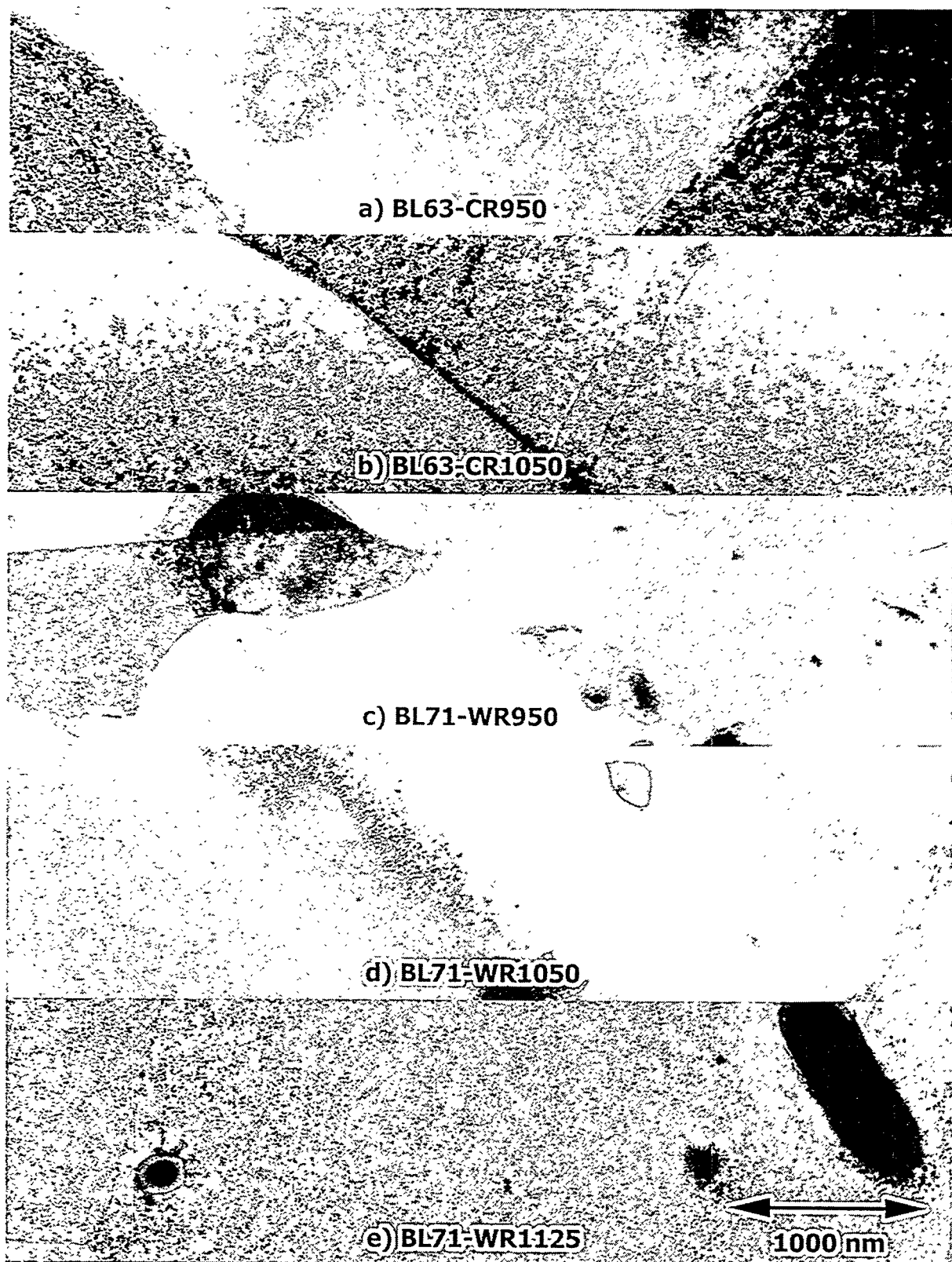


Figure 1. Low magnification examples of microstructures in specimens of V-(4-5%)Cr-(4-5%)Ti irradiated in the X530 experiment.

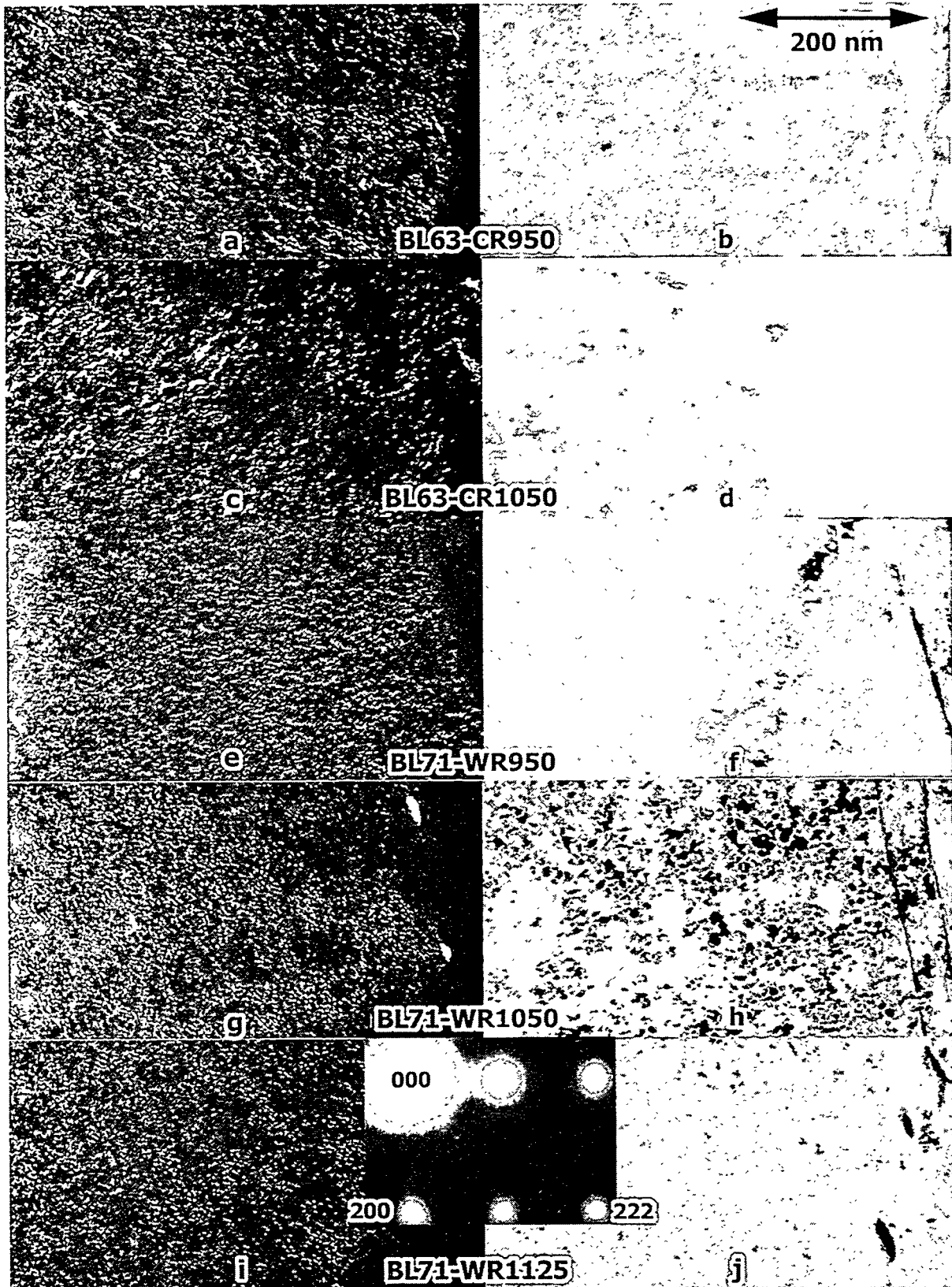


Figure 2. Precipitate dark field and bright field images for specimens of V-(4.5%)Cr-(4.5%)Ti irradiated in the X530 experiment with a (011) diffraction pattern from BL-71-WR1125 inset.

provide any composition dependencies that could be considered characteristic. An effort to identify composition differences at a grain boundary in BL-71-WR1050 were also unsuccessful. Although these efforts will continue within the constraints of available funding, it must be concluded that larger precipitate particles are probably needed to definitively identify the composition of these precipitates.

Discussion

The purpose of this work was to provide an explanation for mechanical property degradation in some heats of V-(4-5%)Cr-(4-5%)Ti. The above results indicate that precipitation during irradiation is probably responsible. Unfortunately, the composition of the precipitate has not yet been established, so that it is not yet possible to provide recommendations for composition modifications for improved properties. This discussion is provided as speculation on the likely causes for the behavior observed.

Several important facts should be first summarized. Table 3 provides postirradiation mechanical properties response² for conditions identical to those examined in this study. From Table 3, it can be shown that BL-63 gave lower levels of both yield strength (YS) and ultimate tensile strength (UTS), but uniform elongation (UE) was similar in comparison with BL-71 following annealing at 950°C, whereas higher annealing temperatures for BL-71 produced lower UE. Total elongation (TE) values followed none of these trends. However, comparison of the compositional differences in Table 1 demonstrates that BL-71 contains less chromium and titanium but higher silicon.

Table 3. Postirradiation mechanical properties for selected specimens in the X530 experiment.

Specimen Designation	Preirradiation heat treatment	0.2% YS (MPa)	UTS (MPa)	UE (%)	TE (%)
BL-63-CR950	cold rolled, annealed at 950°C/1h	701	743	0.8	2.8
BL-63-CR1050	cold rolled, annealed at 1050°C/1h	723	765	1.0	7.0
BL-71-WR950	warm rolled, annealed at 950°C/1h	819	847	0.8	4.1
BL-71-WR1050	warm rolled, annealed at 1050°C/1h	809	818	0.4	6.0
BL-71-WR1125	warm rolled, annealed at 1125°C/1h	880	883	0.2	6.0

Therefore, the experimental observations can be summarized as follows. BL-71 develops more hardening and less uniform elongation following irradiation, BL-71 contains significantly more silicon and a little less chromium and titanium, but the irradiation temperatures are expected to be very similar. Based on this, the likely cause for the observed enhanced hardening would be expected to be precipitation of silicide phases. The observed precipitate particles are very finely distributed, and precipitate number density has been measured for each condition. It can be argued that the particles are larger or more non-uniformly distributed in BL-63, and therefore effectively at lower density (although not supported by quantitative microscopy because distribution is not taken into account), in agreement with the observed hardening behavior.

The diffraction information obtained for this fine precipitation does not straightforwardly correspond to precipitation previously identified in this alloy class. Chung and Smith¹⁰ have provided diffraction information for $Ti_5(Si,P)_3$ and Ti_2O that have similar appearance but different diffraction response. One published diffraction pattern in Figure 2 does show a streak at $\frac{2}{3}\langle 222 \rangle$, but no comment is provided. Chung et al.¹¹ found similar grain boundary contrast in V-4Cr-4Ti irradiated at 425°C to 31 dpa in the DHCE experiment but ruled out Ti_5Si_3 precipitation. Chung, Loomis, and Smith¹² showed

microstructures in irradiated V-4Cr-4Ti containing Ti_5Si_3 , but provided no diffraction information. Satou et al.¹³ showed diffraction and dark field images of Ti_5Si_3 precipitates in V-5Ti-5Cr-1Si-Al following irradiation at 520°C, but the diffraction information is not in agreement with the present findings. Gelles and Chung¹⁴ found precipitation in V-5Cr-5Ti following irradiation with a diffraction streak at $\frac{3}{4}\langle 200 \rangle$, but compositional information was not obtained and it was "anticipated that the phase was TiP, but similar morphologies have been identified previously as Ti_5Si_3 ." Chung et al.¹⁵ again published a grain boundary image in V-4Cr-4Ti irradiated at 425°C to 31 dpa similar to those in Figure 2. Finally, Fukumoto et al.¹⁶ showed dark field images of similar features in V-4Cr-4Ti following irradiation but identify them as titanium oxide, Ti_2O or TiO_x ($x < 0.5$) without giving any diffraction information. From these analyses it appears that the precipitate found in the present work cannot be identified as a silicide based on diffraction information, whereas it may be, but has not definitively been shown to be, an oxide or a phosphide. If an oxide is responsible for the hardening found in the X530 experiment, then differences in heat-to-heat response could best be explained by a consequence of variation in irradiation temperature and not composition. However, as noted in Table 2, due to capsule radial positions, negligible differences are expected.⁷ A phosphide cause for embrittlement is unlikely because phosphorus levels are low in BL-71.⁴ The most critical experiment continues to be identification of the phase in BL-71 that causes the diffraction streaks at $\frac{3}{4}\langle 200 \rangle$ and $\frac{2}{3}\langle 222 \rangle$.

CONCLUSIONS

Five specimen conditions from the X530 experiment, comprising two heats of V-(4-5%)Cr-(4-5%)Ti given different preirradiation heat treatments and directly corresponding to tested mechanical properties specimens, have been examined to identify the cause of irradiation hardening. It is found that hardening is at least in part due to precipitation of a high density of small particles. However, analytical electron microscopy was unable to provide precipitate composition and it is not yet possible to provide an explanation for the differences in response between the heats.

FUTURE WORK

This work will be continued within the confines of funding and specimen availability.

REFERENCES

1. B. A. Loomis, A. B. Hull, and D. L. Smith, *J. Nucl. Mater.*, **179-181** (1992) 148.
2. S. J. Zinkle, D. J. Alexander, J. P. Robinson, L. L. Snead, A. F. Rowcliffe, L. T. Gibson, W. S. Eatherly and H. Tsai, DOE/ER-0313/21, 73.
3. H. M. Chung, J. Gazda, L. J. Nowicki, J. E. Sanecki, and D. L. Smith, DOE/ER-0313/15, 207.
4. H. M. Chung, H. Tsai, D. L. Smith, K. Peterson, C. Curtis, C. Wojcik, and R. Kinney, DOE/ER-0313/17, 178.
5. H. Tsai, V. Strain, A. G. Hins, H. M. Chung, L. J. Nowicki, and D. L. Smith, DOE/ER-0313/17, 8.
6. H. Tsai, V. Strain, A. G. Hins, H. M. Chung, L. J. Nowicki, and D. L. Smith, DOE/ER-0313/18, 85.

7. Personal communication from Bob Strain, ANL: "A more refined thermal analysis of the X530 experiment shows that the centerline temperature for subcapsule S8 to be 400.5°C and that for S9 to be 399.1°C. The subcapsule inside surface temp was ~1.5°C lower, in both cases. S8, at a higher axial elevation, ordinarily would have a higher temperature. But the capsule it was in, AH2, was located at the the center of the hex, thus receiving less heat from the neighboring (hotter) subassemblies. The two countervailing effects essentially cancelled out."
8. Personal communication from L. W. Greenwood, PNNL, recommending that an extra column be added to table 3, DOE/ER-031/21, page 228, headed dpa (vanadium) and reading 14.0, 31.0, 38.1, 29.3, 15.4, 6.36.
9. D. S. Gelles and Huaxin Li, DOE/ER-0313/19, 22.
10. H. M. Chung and D. L. Smith, J. Nucl. Mater., 191-194 (1992) 942.
11. H. M. Chung, L. J. Nowicki, J. Gazda, and D. L. Smith, DOE/ER-0313/17, 211.
12. H. M. Chung, B. A. Loomis, and D. L. Smith, J. Nucl. Mater., 212-215 (1994) 804.
13. M. Satou, K. Abe, and H. Kayano, IBID, 794.
14. D. S. Gelles and H. M. Chung, DOE/ER-0313/21, 79.
15. H. M. Chung, B. A. Loomis, and D. L. Smith, J. Nucl. Mater., 233-237 (1996) 466.
16. K. Fukumoto, H. M. Chung, J. Gazda, D. L. Smith, and H. Matsui, "Helium Behavior in Vanadium-Based Alloys Irradiated in the Dynamic Helium Charging Experiments," presented at the 18th ASTM International Symposium on Effects of Radiation on Materials, held June 1996 in Hyannis, MA, to be published.